

Supporting Information

Cyclometalated iridium(III) complexes with imidazo[4,5-f][1,10]phenanthroline derivatives for mitochondrial imaging in living cells

Chengzhi Jin, Jiangping Liu, Yu Chen, Guanying Li, Ruilin Guan, Pingyu Zhang,
Liangnian Ji and Hui Chao*

MOE key laboratory of Bioinorganic and Synthetic Chemistry, School of Chemistry and Chemical
Engineering, Sun Yat-Sen University, Guangzhou 510275, P. R. China

E-mail: ceschh@mail.sysu.edu.cn

Fig. S1 ES-MS spectra of Mito-Ir1 in CH ₃ OH solutions	S3
Fig. S2 ¹ HNMR spectra of Mito-Ir1 in DMSO- <i>d</i> 6	S3
Fig. S3 ES-MS spectra of Mito-Ir2 in CH ₃ OH solutions	S4
Fig. S4 ¹ HNMR spectra of Mito-Ir2 in DMSO- <i>d</i> 6	S4
Fig. S5 ES-MS spectra of Mito-Ir3 in CH ₃ OH solutions	S5
Fig. S6 ¹ HNMR spectra of Mito-Ir3 in DMSO- <i>d</i> 6	S5
Fig. S7 ES-MS spectra of Mito-Ir4 in CH ₃ OH solutions	S6
Fig. S8 ¹ HNMR spectra of Mito-Ir4 in DMSO- <i>d</i> 6	S6
Fig. S9 ES-MS spectra of Mito-Ir5 in CH ₃ OH solutions	S7
Fig. S10 ¹ HNMR spectra of Mito-Ir5 in DMSO- <i>d</i> 6	S7
Fig. S11 ES-MS spectra of Mito-Ir6 in CH ₃ OH solutions	S8
Fig. S12 ¹ HNMR spectra of Mito-Ir6 in DMSO- <i>d</i> 6	S8
Fig. S13 ES-MS spectra of Mito-Ir7 in CH ₃ OH solutions	S9
Fig. S14 ¹ HNMR spectra of Mito-Ir7 in DMSO- <i>d</i> 6	S9
Fig. S15 Absorption spectra of Mito-Ir1-Ir7	S10
Fig. S16 Emission spectra of Mito-Ir1-Ir6	S10
Fig. S17 Distribution analysis of Mito-Ir1-Ir7 in HeLa cells by ICP-MS	S11
Fig. S18 Time-dependent cell uptake of Mito-Ir7 by ICP-MS.....	S11
Fig. S19 Photobleaching experiments of Mito-Ir1 in HeLa cells.....	S12
Fig. S20 Photobleaching experiments of Mito-Ir2 in HeLa cells.....	S12
Fig. S21 Photobleaching experiments of Mito-Ir3 in HeLa cells.....	S13
Fig. S22 Photobleaching experiments of Mito-Ir4 in HeLa cells.....	S13

Fig. S23 Photobleaching experiments of Mito-Ir5 in HeLa cells.....	S14
Fig. S24 Photobleaching experiments of Mito-Ir6 in HeLa cells.....	S14
Fig. S25 Flow cytometric histogram profile of cellular uptake of Mito-Ir7 in HeLa cells.	S15
Fig. S26 Emission intensity of Mito-Ir1-Ir7 at 595 nm under different pH	S16
Table S1 Photophysical data of Mito-Ir1-Ir7	S16

Peak#1 Ret.Time:Averaged 1.017-1.050(Scan#62-64)
 BG Mode:Calc 0.950<->1.200(58<->73)
 Mass Peaks:456 Base Peak:797.35(288503) Polarity:Pos Segment1 - Event1

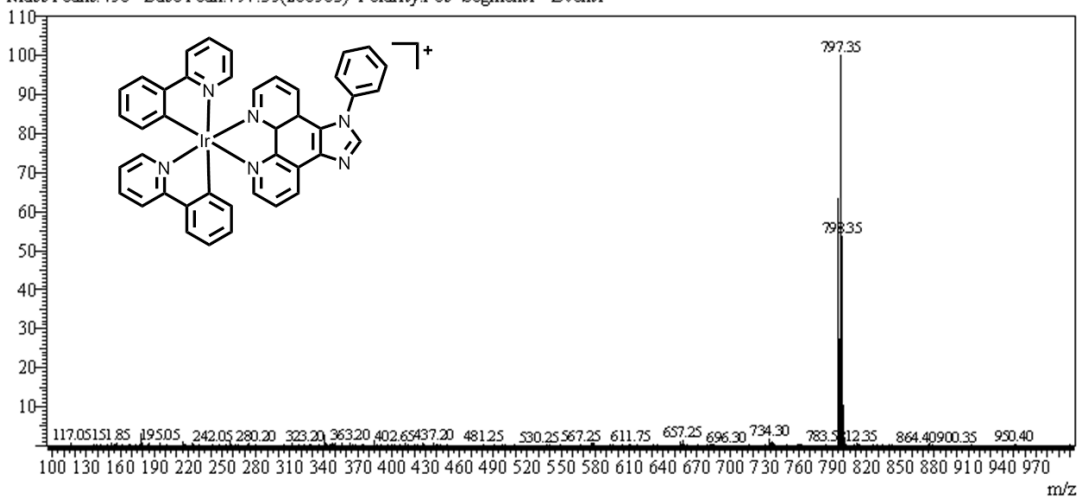


Fig. S1 ES-MS spectra of **MitoIr1** in CH_3OH solutions.

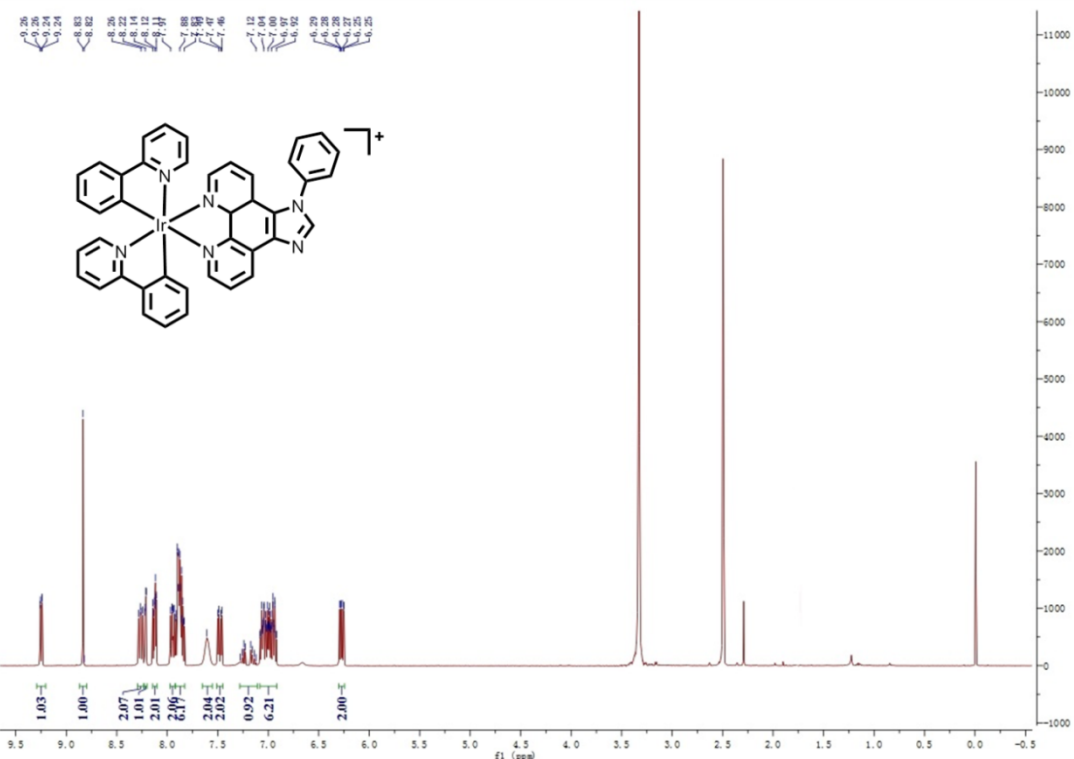


Fig. S2 ^1H NMR spectra of **MitoIr1** in DMSO-d_6 , 500 MHz.

Peak# 1 Ret. Time:Averaged 5.983-6.017(Scan#:360-362)
 BG Mode:Calc 5.883<->6.083(354<->366)
 Mass Peaks:368 Base Peak:811.35(290311) Polarity:Pos Segment1 - Event1

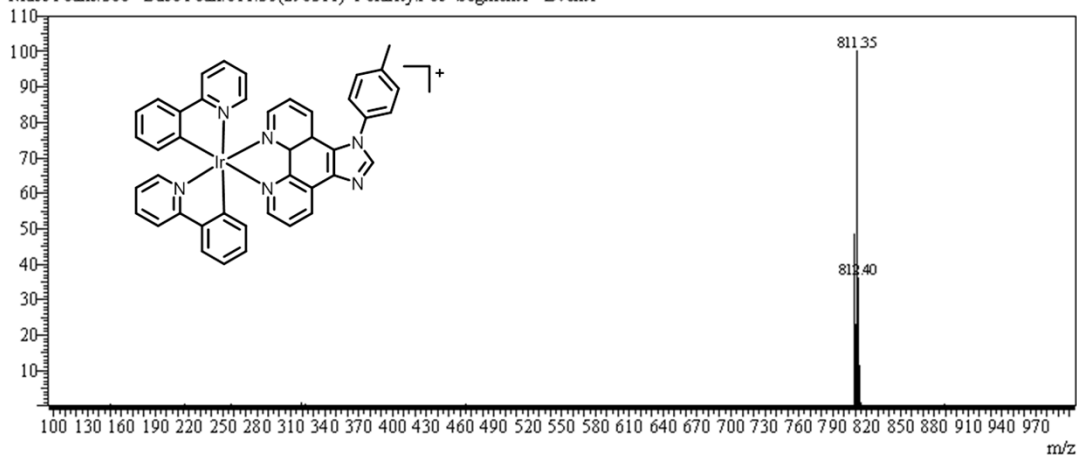


Fig. S3 ES-MS spectra of **MitoIr2** in CH_3OH solutions.

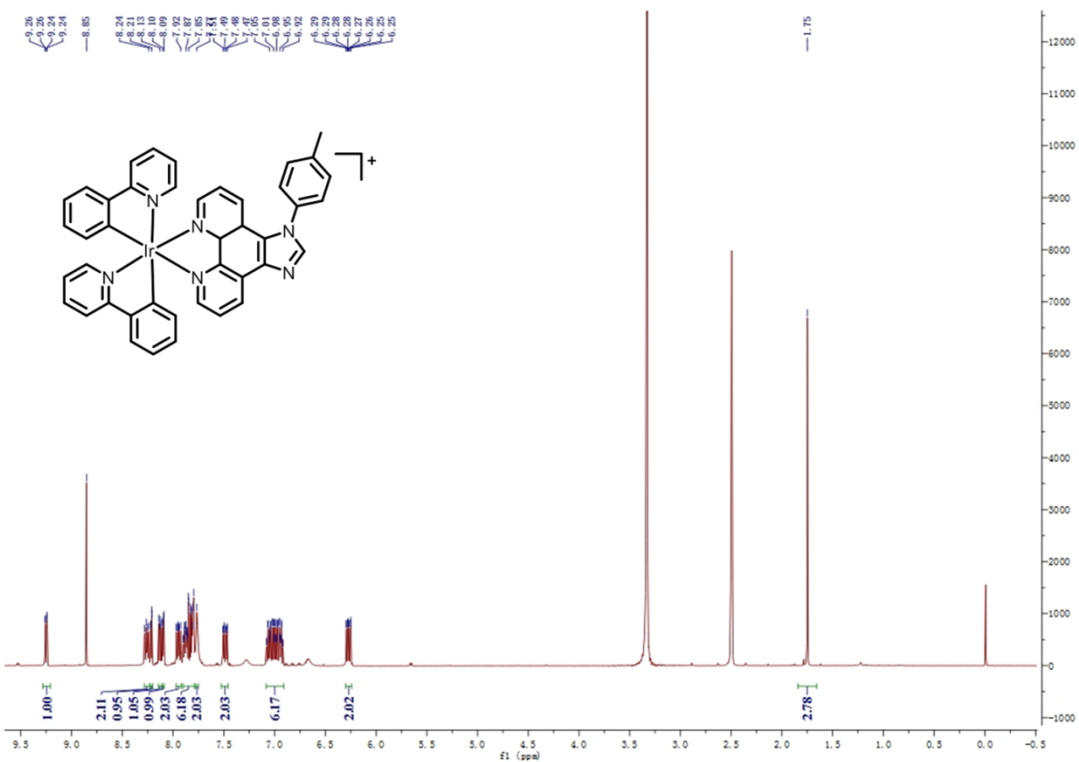


Fig. S4 ^1H NMR spectra of **MitoIr2** in DMSO-d_6 , 500 MHz.

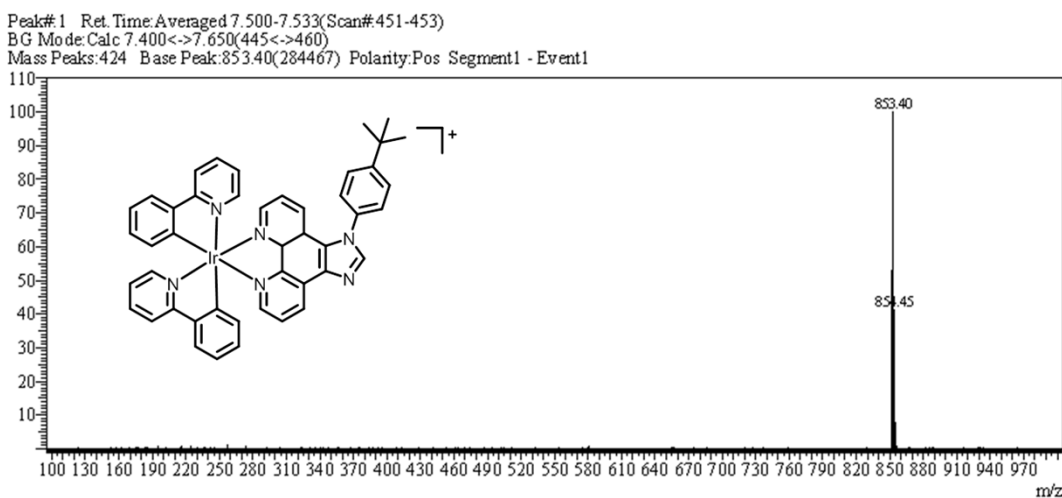


Fig. S5 ES-MS spectra of MitoIr3 in CH₃OH solutions.

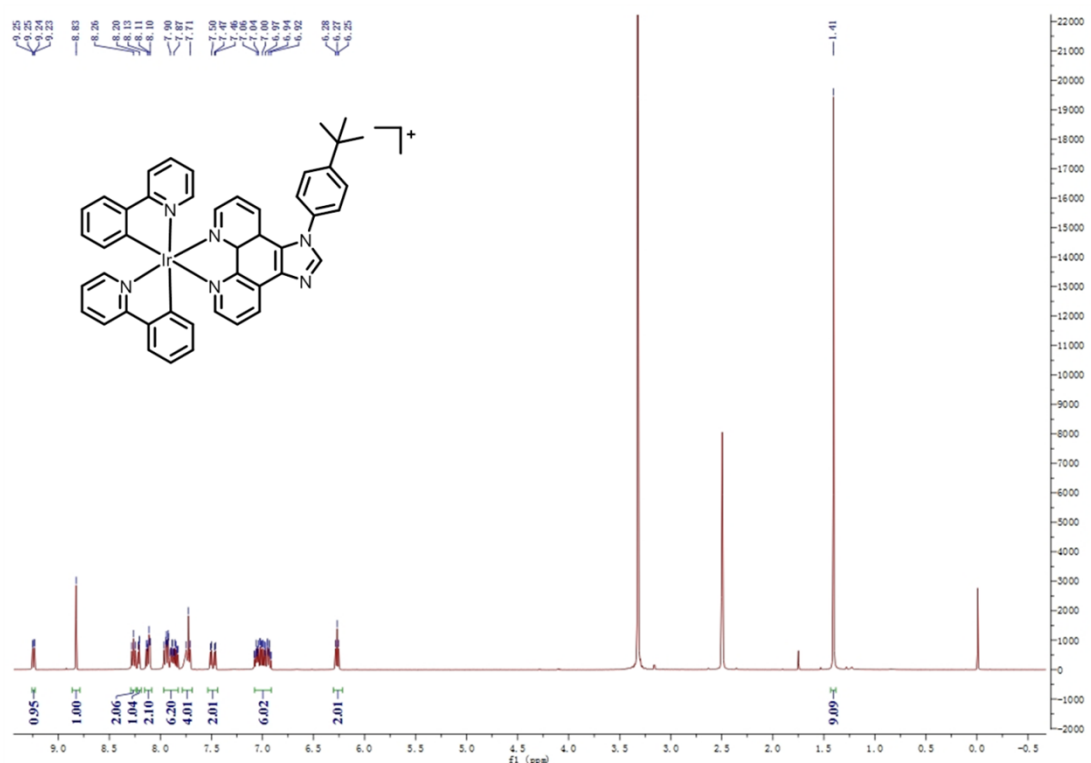


Fig. S6 ^1H NMR spectra of MitoIr3 in DMSO-d₆, 500 MHz.

Peak#1 Ret.Time:Averaged 11.550-11.583(Scan# 694-696)
 BG Mode:Calc 11.500<->11.700(691<->703)
 Mass Peaks:378 Base Peak:815.35(298581) Polarity:Pos Segment1 - Event1

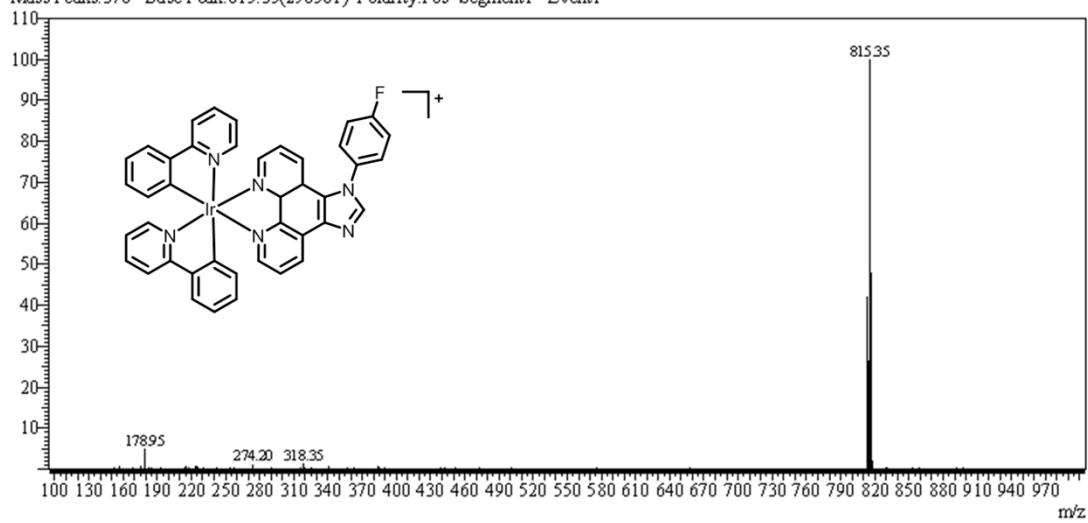


Fig. S7 ES-MS spectra of **MitoIr4** in CH_3OH solutions.

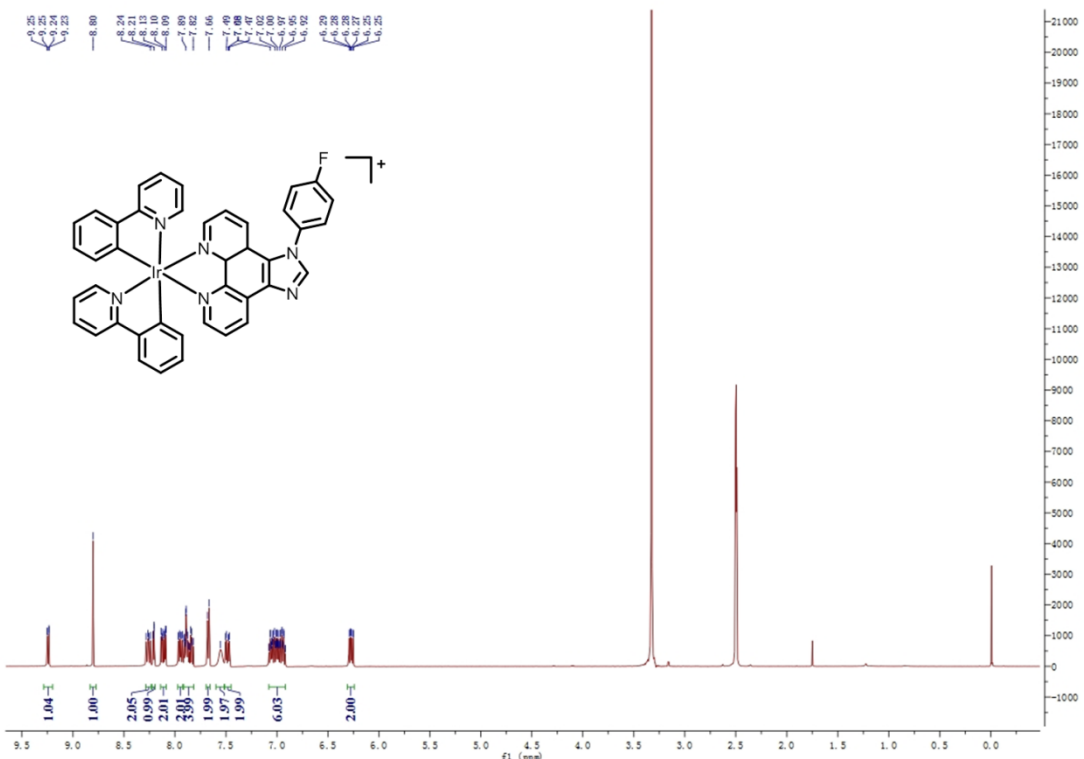


Fig. S8 ^1H NMR spectra of **MitoIr4** in DMSO-d_6 , 500 MHz.

Peak#1 Ret.Time:Averaged 12.933-12.967(Scan#777-779)
 BG Mode:Calc 12.800<->13.167(769<->791)
 Mass Peaks:366 Base Peak:827.35(331709) Polarity:Pos Segment1 - Event1

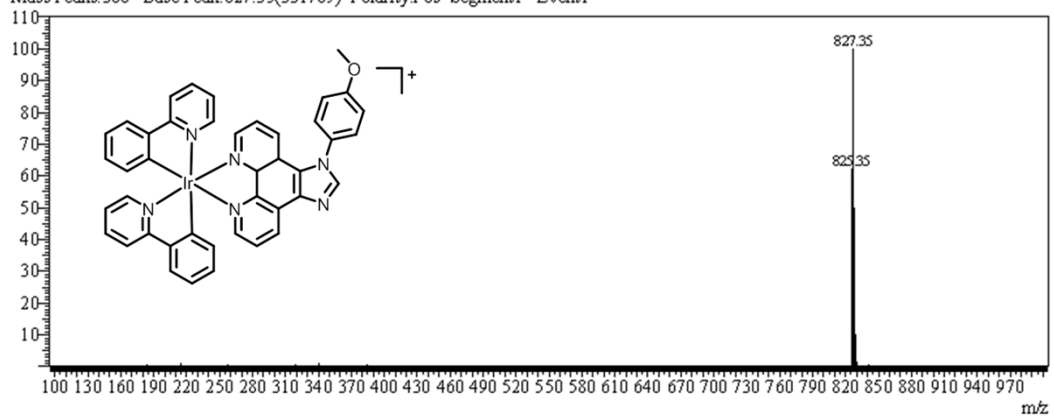


Fig. S10 ¹H NMR spectra of MitoIr5 in DMSO-d₆, 500 MHz.

Peak#1 RetTime:Averaged 9.933-9.967(Scan#:597-599)
 BG Mode:Calc 9.850<->10.083(592<->606)
 Mass Peaks:430 Base Peak:840.35(38264) Polarity:Pos Segment1 - Event1

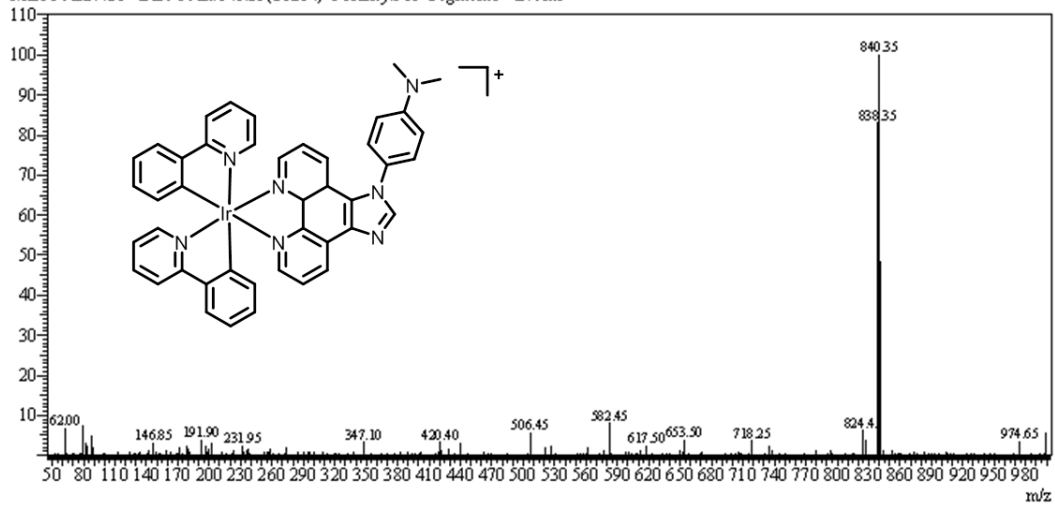


Fig. S11 ES-MS spectra of **MitoIr6** in CH_3OH solutions.

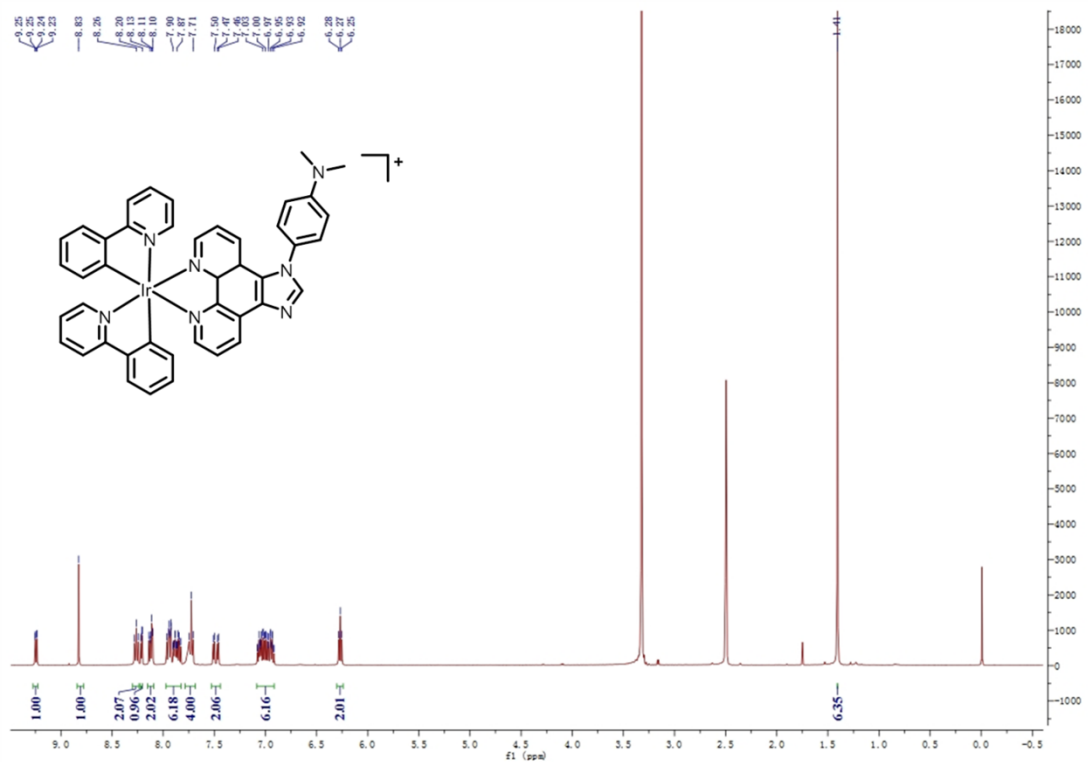


Fig. S12 ^1H NMR spectra of **MitoIr6** in DMSO-d_6 , 500 MHz.

Peak#:1 Ret.Time:Averaged 27.217-27.250(Scan#1634-1636)
 BG Mode:Calc 27.100<->27.317(1627<->1640)
 Mass Peaks:447 Base Peak:889.35(215322) Polarity:Pos Segment1 - Event1

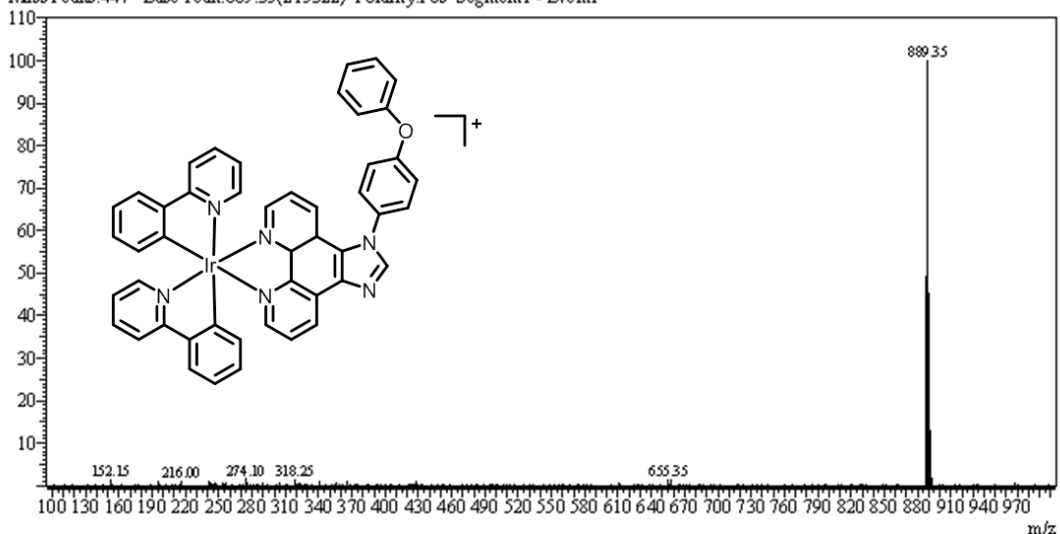


Fig. S13 ESI-MS spectra of **MitoIr7** in CH₃OH solutions.

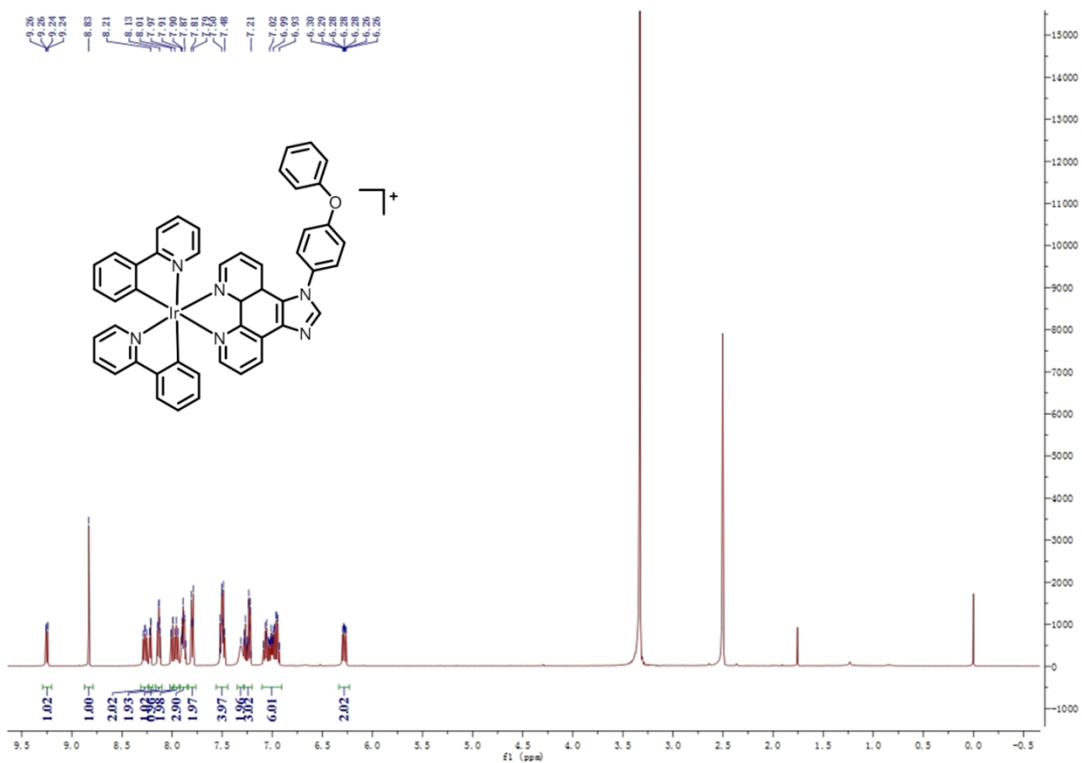


Fig. S14 ¹H NMR spectra of **MitoIr7** in DMSO-d₆, 500 MHz.

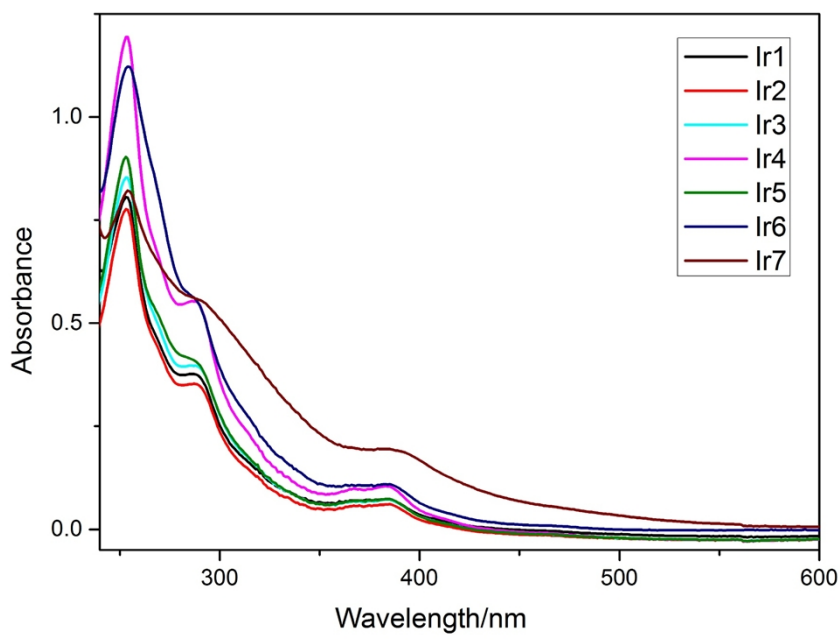


Fig. S15 Absorption spectra of **MitoIr1-MitoIr7** (10 μM) in a DMSO/PBS (v/v = 1:999) solution at 298K.

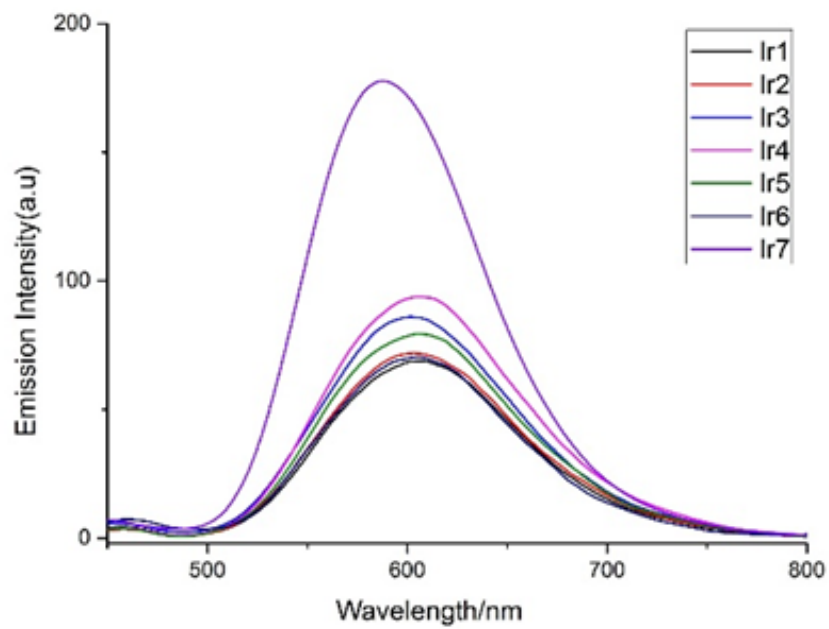


Fig. S16 Emission spectra of **MitoIr1-MitoIr6** (10 μM) and **MitoIr7** (2 μM) in a DMSO/PBS (v/v = 1:999) solution at 298K with an excitation wavelength of 384 nm.

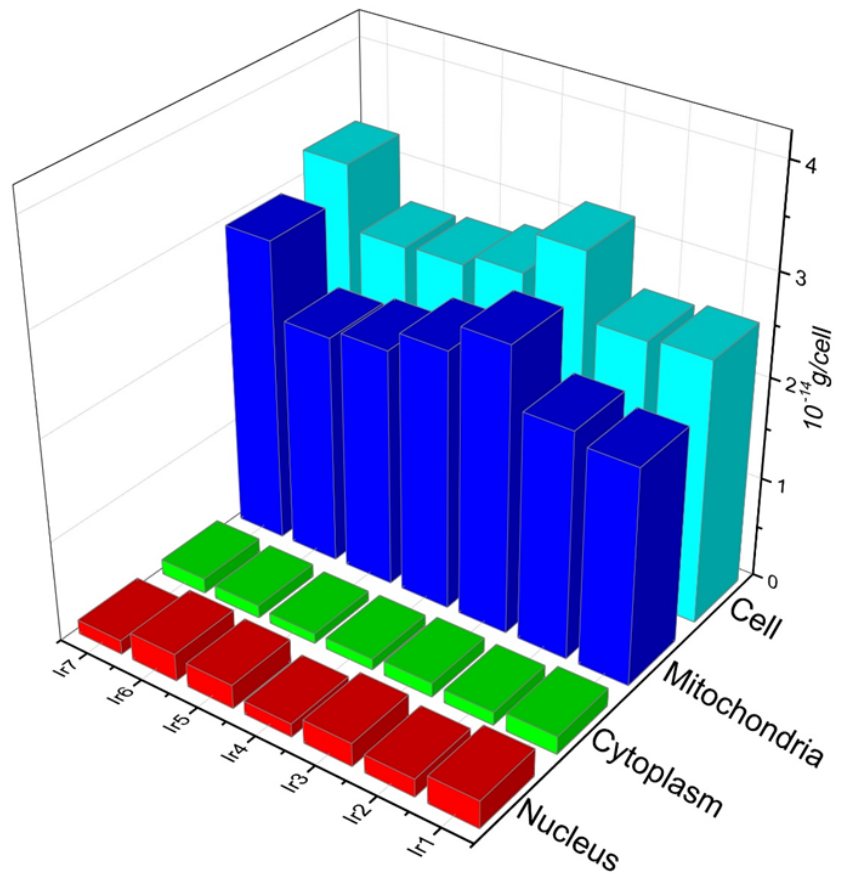


Fig. S17 Distribution analysis of **MitoIr1–MitoIr7** in HeLa cells by ICP-MS.

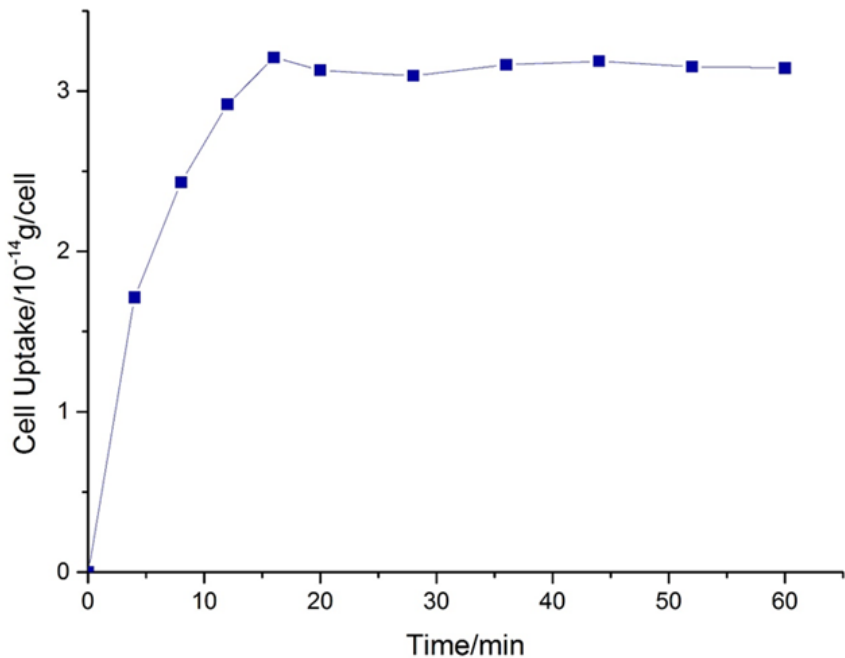


Fig. S18 Time-dependent cell uptake of **MitoIr7** by ICP-MS.

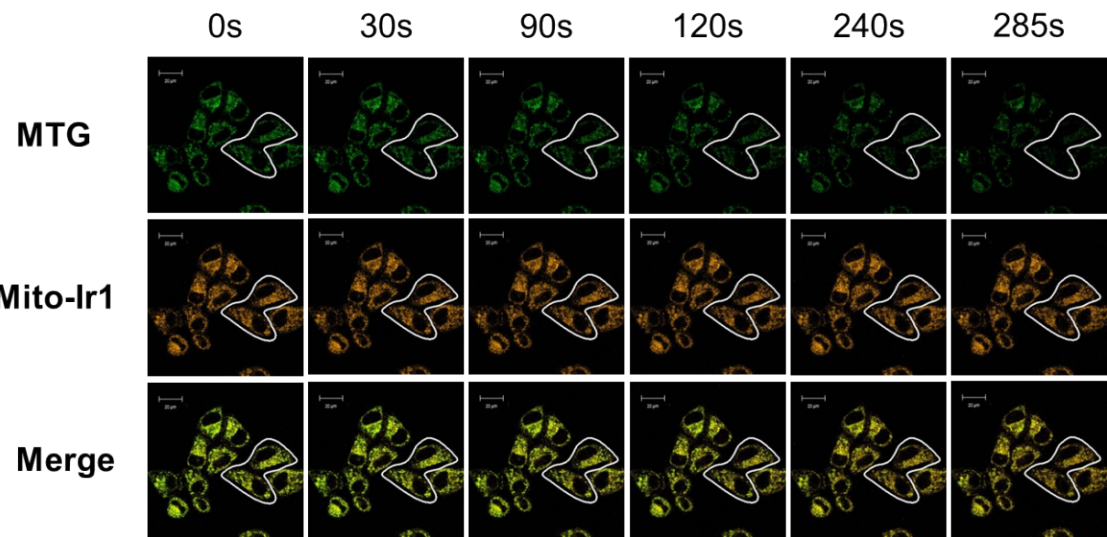


Fig. S19 Photobleaching experiments of MitoIr1 in HeLa cells.

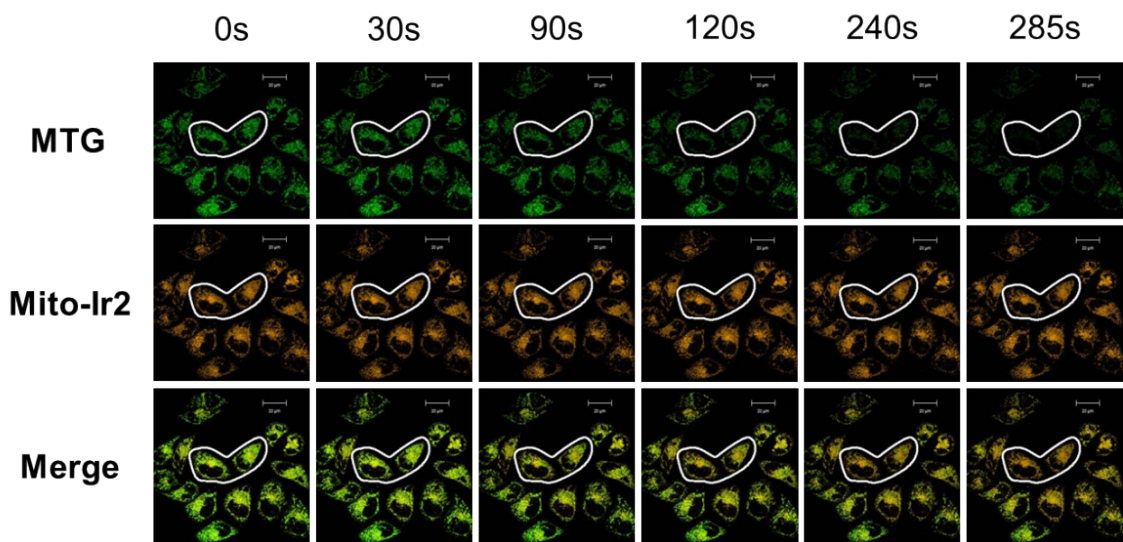


Fig. S20 Photobleaching experiments of MitoIr2 in HeLa cells.

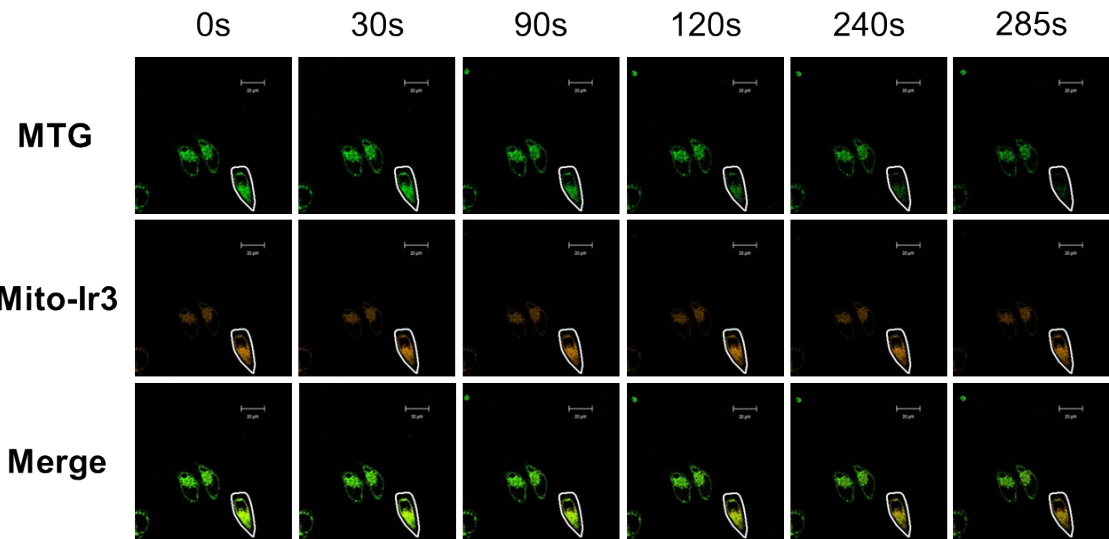


Fig. S21 Photobleaching experiments of MitoIr3 in HeLa cells.

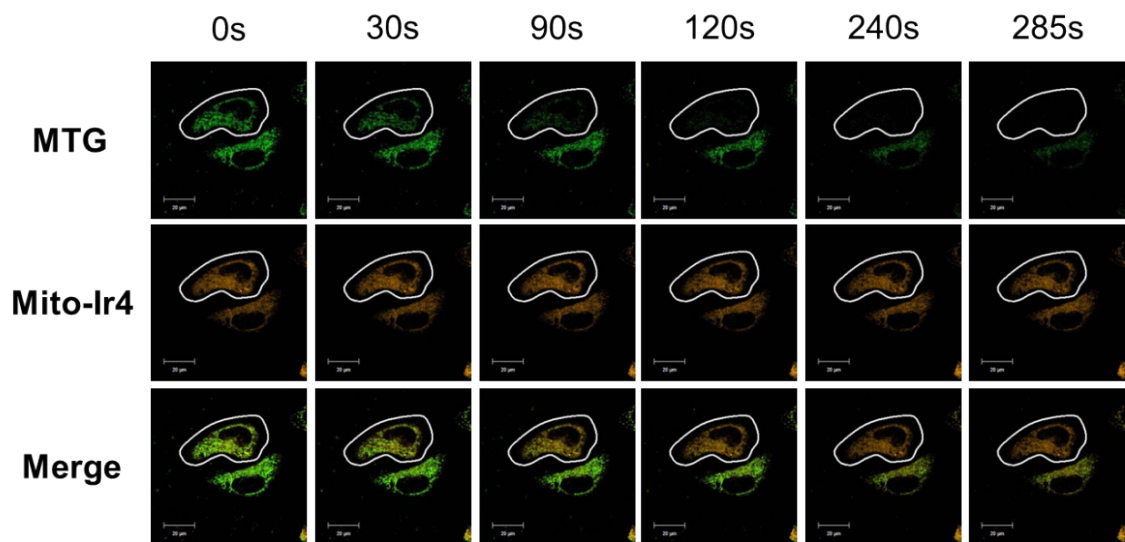


Fig. S22 Photobleaching experiments of MitoIr4 in HeLa cells.

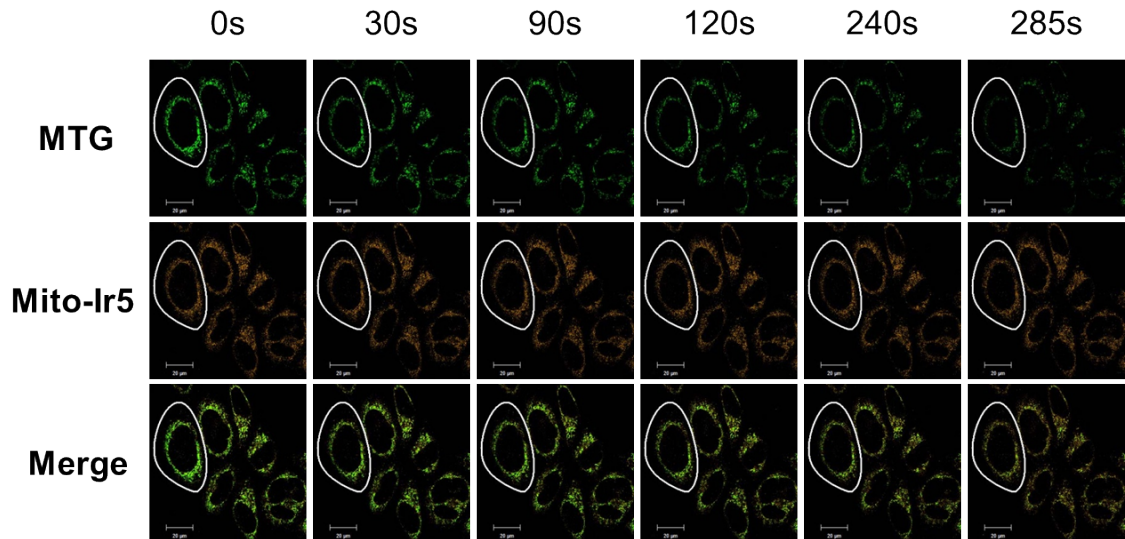


Fig. S23 Photobleaching experiments of MitoIr5 in HeLa cells.

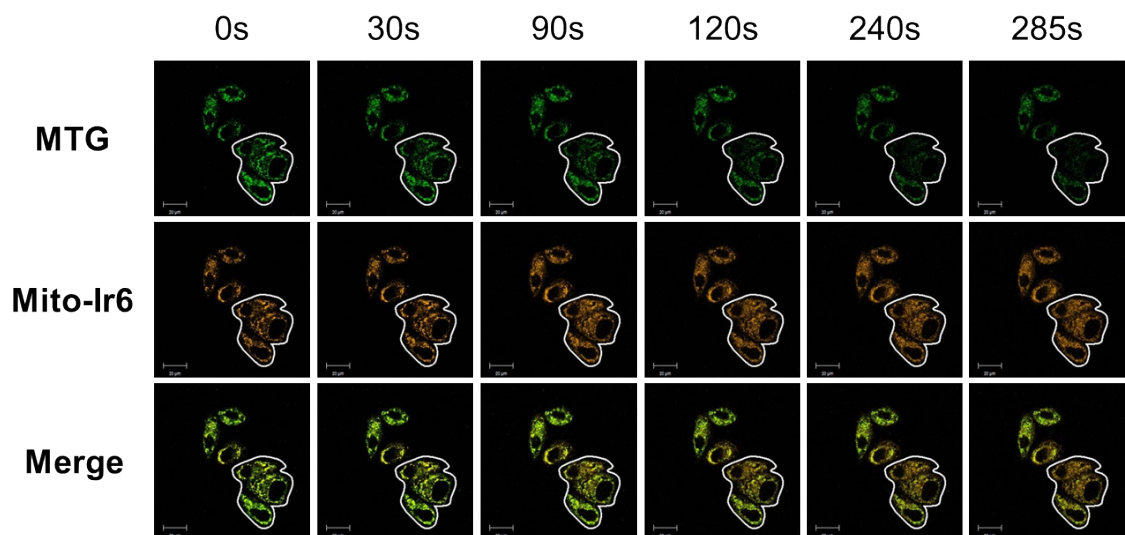


Fig. S24 Photobleaching experiments of MitoIr6 in HeLa cells.

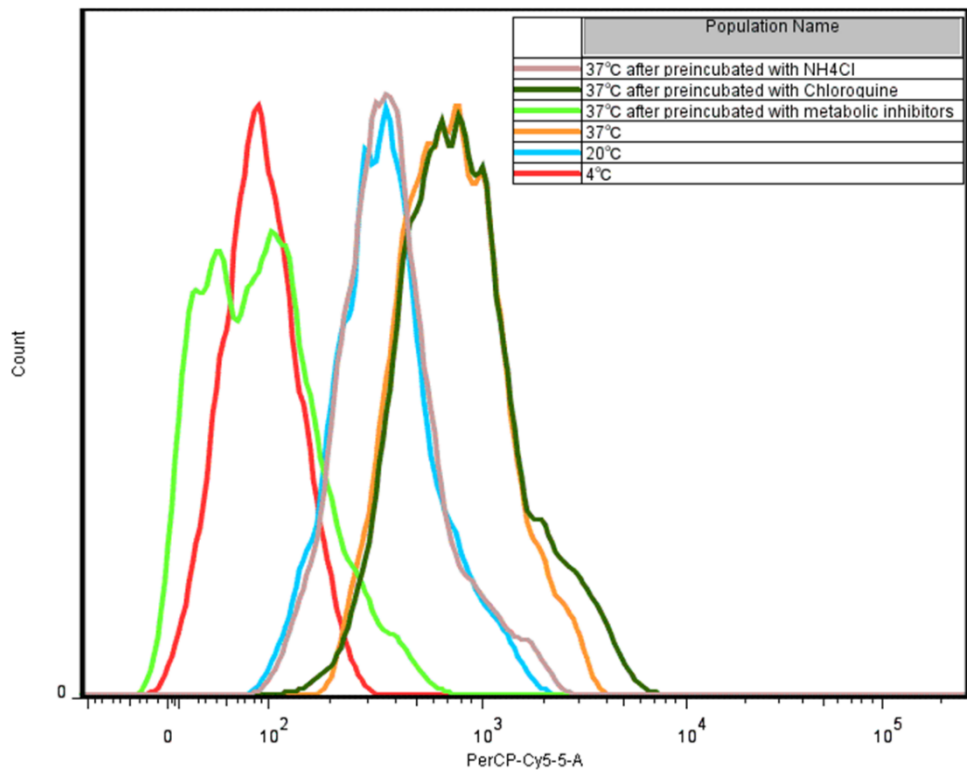


Fig. S25 Flow cytometric histogram profile of cellular uptake of **MitoIr7** in HeLa cells. HeLa cells were incubated with 0.5 μ M **MitoIr7** for 15 min at 37 °C (orange), 20°C (light blue), 4 °C (red), and 37 °C after the cells were preincubated with metabolic inhibitors 2-deoxy-D-glucose (50 mM) and oligomycin (5 μ M) in PBS for 1 h at 37°C (light green), endocytic inhibitors NH₄Cl (50 mM) (light purple) and chloroquine (50 μ M) (dark green) in PBS for 1 h at 37°C, respectively.

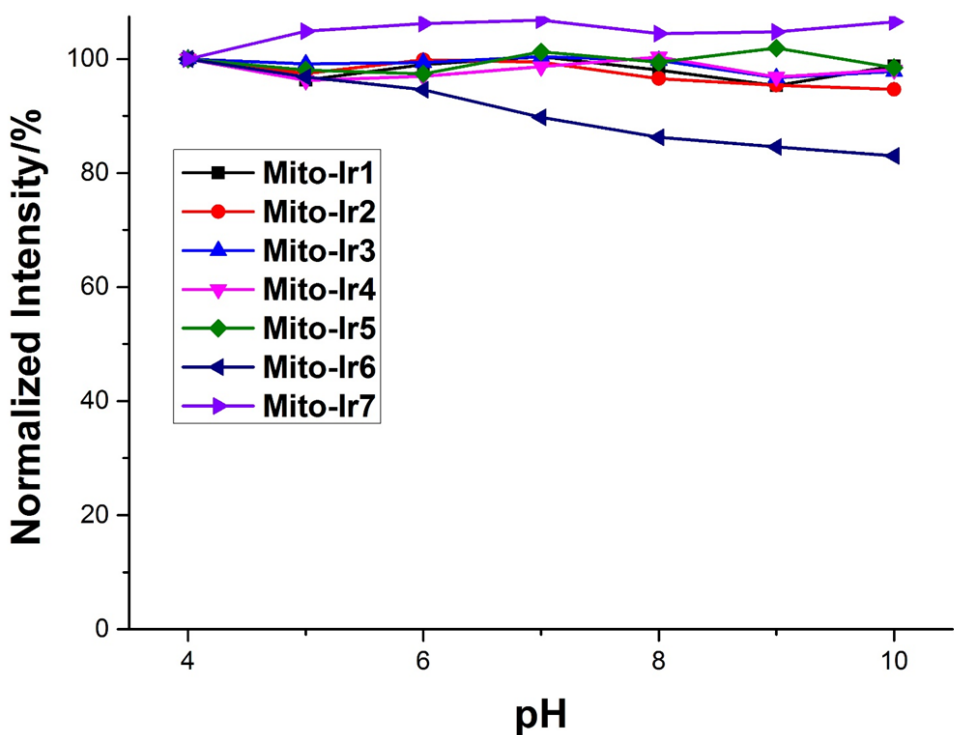


Fig. S26 Emission intensity of 5 μM **MitoIr1-MitoIr7** at 595 nm under different pH in a Britton-Robinson buffer.

Table S1 Photophysical data of **MitoIr1-MitoIr7**.

Complexes	$\lambda_{\text{abs}}/\text{nm}$	$\lambda_{\text{em}}/\text{nm}$	τ/ns	Φ
Ir1	253, 286, 383	598	94.5	0.108
Ir2	253, 287, 384	599	90.7	0.221
Ir3	253, 288, 383	596	85.9	0.219
Ir4	254, 288, 383	597	85.2	0.098
Ir5	253, 383	593	89.3	0.216
Ir6	254, 382	594	93.0	0.057
Ir7	288, 254, 383	590	91.2	0.365